Non-Fermi-liquid fixed point in multi-orbital Kondo impurity model relevant for Hund's metals

Alen Horvat,[1] Rok Žitko,[1,2] and Jernej Mravlje[1]

[1] *Jozef Stefan Institute, Jamova 39, SI-1000, Ljubljana, Slovenia*
[2] *University of Ljubljana, Faculty of Mathematics and Physics, Jadranska 19, Ljubljana, Slovenia*

(Dated: July 17, 2019)

Due to the separation between the spin and the orbital screening scales, the normal state of Hund's metals at ambient temperature can be loosely characterized as a partially coherent state with fluctuating spins and quenched orbital moments. With the aim to characterize this situation more precisely, we investigate the Kondo-Kanamori impurity model that describes the low-energy local physics of three-orbital Hund's metals occupied by two or four electrons. Within this model one can diminish the mixed spin-orbital terms and thereby enhance the separation between the two screening scales, allowing a more precise investigation of the intermediate state. Using the numerical renormalization group we calculate the impurity entropy as well as the temperature and frequency dependence of the spin and the orbital susceptibilities. We uncover a non-Fermi-liquid two-channel overscreened SU(3) fixed point that controls the behavior in the intermediate regime. We discuss its fingerprints in the frequency dependence of local orbital susceptibility and the shape of the spectral function.

Ruthenates exhibit remarkable properties such as bad-metallic behavior at high temperatures, a small value of temperature below which a Fermi-liquid behavior is observed in measurements of transport [1], and unusual optical response [2–6]. Ruthenates have four electrons in the t_{2g} shell of extended 4d orbitals that experience only moderate Coulomb repulsion, hence the occurrence of correlation was considered mysterious [3]. The dynamical mean-field theory (DMFT) [7] calculations that map the bulk problem to a problem of a quantum impurity in an effective bath have related the occurrence of the low coherence scale to strong electronic correlations that are caused by the Hund's coupling [6, 8, 9]. The same Hund's physics applies also to iron pnictides [10, 11]. A term "Hund's metals" has been introduced to describe ruthenates, iron pnictides, as well as related compounds [12], and a term Hund's impurity was proposed for multiorbital impurities on metallic hosts [13].

A successful line of thinking associates the correlations in Hund's metals with the proximity to a half-filled Mott insulator [14–17]: the Hund's coupling favors large spin and blocks charge fluctuations of the half filled ground state. A different and equally successfully line of thinking considers Hund's metals in terms of the low-energy Kondo physics of the effective impurity model obtained by the DMFT mapping, which is a subject this paper will elaborate on, too. This point of view is based on the observation that the Hund's coupling suppresses the spin-coherence temperature [18–25]. This scale suppression is related to a reduced Kondo coupling constant for the spin degree of freedom that occurs because the Hund's interaction favors those charge fluctuations where the added electron is parallel, which competes with the usual antiferromagnetic Kondo coupling driven by the Pauli principle. The orbital-Kondo couplings are, meanwhile, not affected by the Hund's coupling [18, 19, 21]. The Hund's coupling hence leads to a distinct Kondo screening scale for spins and orbitals, T_K^S, T_K^L, respectively, which was first suggested in Ref. [26].

The intermediate-temperature state where $T_K^S < T < T_K^L$ has been characterized in the literature [18–25] as a state with fluctuating spins with a Curie dependence of spin susceptibility, $\chi_S \propto 1/T$, and quenched orbitals with constant orbital susceptibility, $\chi_L \sim$ const. Despite the scale separation the spins and the orbitals are not fully independent because of the mixed spin-orbital coupling terms J_{ls} (see below for a precise definition). The Hund's metals are, in fact, characterized by a slow two-stage crossover to a fully screened Fermi liquid. It is a key question whether the intermediate state can be characterized in a more precise way and what is the expected behavior of the observables. Namely, within the DMFT picture the solid is a collection of atoms having some high-energy multiplets that are self-consistently screened/quenched as we flow to low energy. The key issue here is whether during that flow one passes close to some non-trivial fixed point (and what that fixed point is) or whether one goes directly into the Fermi liquid ground state.

To address this, in this paper we consider a Kondo model relevant to a Hund's impurity. This allows us to suppress J_{ls} and separate the spin- and the orbital screening scales far from each other. In the intermediate temperature regime we reveal a non-Fermi liquid behavior that can be associated to an overscreened two-channel SU(3) fixed point. The orbital susceptibility behaves with frequency as $\omega^{1/5}$ in this regime. We discuss also the implications of this regime for the shape of the spectral function and discuss the relevance of our findings for the physics of Hund's metals.

The relevance of non-Fermi-liquid physics for the ruthenates within the DMFT description was first dis-

cussed in Ref. [27]. In contrast to that paper that suggested the non-Fermi-liquid physics to persist to zero temperature, which turned out not to be the case, we stress that the NFL physics revealed here applies to the incoherent regime, only.

Multi-orbital impurities with largely quenched orbital degrees of freedom but fluctuating spins are equally relevant in the context of magnetic adsorbates on surfaces. These can be probed at the single-atom level using scanning tunneling microscopy and spectroscopy, providing a direct way of probing local non-Fermi-liquid phenomena through characteristic spectral features [13, 28].

Model and methods – We study the three-orbital impurity occupied by two electrons. The Anderson interaction term reads

$$H_{\rm int} = (U-3J)\frac{\hat{N}(\hat{N}-1)}{2} - 2J\mathbf{S}^2 - \frac{1}{2}J\mathbf{L}^2. \quad (1)$$

Here U is the Coulomb repulsion, J the Hund's coupling, $\hat{N}$ the charge operator, $\mathbf{S}$ the spin operator and $\mathbf{L}$ the orbital angular momentum operator. Eliminating the charge fluctuations and taking into account that Hund's rule coupling binds the two electrons at the impurity into a spin $S=1$ and orbital momentum $L=1$ object, this model maps onto a Kondo Hamiltonian

$$H_K = H_0 + J_s\mathbf{S}\cdot\sigma + J_l\mathbf{L}\cdot\mathbf{l} + J_q\mathbf{Q}\cdot\mathbf{q} + J_{ls}(\mathbf{L}\otimes\mathbf{S})\cdot(\mathbf{l}\otimes\sigma) + J_{qs}(\mathbf{Q}\otimes\mathbf{S})\cdot(\mathbf{q}\otimes\sigma) + J_p n. \quad (2)$$

where $\mathbf{S},\mathbf{L},\mathbf{Q}$ are respectively the impurity spin, orbital, orbital-quadrupole operators and $\mathbf{s},\mathbf{l},\mathbf{q}$ are the corresponding operators for bath electrons at the position of the impurity, and n is their charge (J_p is the potential scattering parameter). The five quadrupole operators $\mathbf{Q}$ are second order orbital tensor operators defined as $Q^{bc}_{i,j} = \left(L^b_{i,m}L^c_{m,j} + L^c_{i,m}L^b_{m,j}\right)/2 - \frac{2}{3}\delta_{b,c}\delta_{i,j}$ for $bc = 11, 12, 13, 23, 33$. The three-orbital conduction band is described by H_0 and assumed flat with its half-bandwidth $D=1$ taken as the energy unit. The parameters of the Kondo Hamiltonian can be obtained from the Anderson model by the Schrieffer-Wolff approximation [21]. In the paper, we consider values of the Kondo parameters $J_p = 0.0044, J_s = 0.025, J_l = 0.033, J_q = 0.035, J_{ls} = 0.059, J_{qs} = 0.055$ that correspond to an Anderson-Kanamori model with $U = 3.2, J = 0.4$ and hybridization function $\Gamma = 0.1$ at the occupancy of $N = 2$ electrons. We will refer to the Kondo model with those parameters as the "realistic Kondo model". In order to reveal the interesting physics we will also relax the parameters from these values as described in the captions of the corresponding plots.

We solved the model Eq. (2) with the numerical renormalization group (NRG) method [29–31]. We took $\Lambda = 5$ and kept up to 3000 states in the diagonalization. We verified that increasing this number to 4000 and/or varying the value of Λ does not affect the results appreciably. We used the z-interleaving with 8 different choices of z.

RG equations – The Hamiltonian has been studied by perturbative renormalization group (RG) in Ref. 21. One of the main results from that work is that under the RG flow the difference between quadrupole and orbital coupling constants becomes unimportant at low energies, that is $J_{ls}/J_{qs} \to 1$, $J_l/J_q \to 1$, and the physics becomes that of the problem with higher SU(3) orbital symmetry [19, 21].

The RG equations to lowest order for a flat density of states (additionally, for brevity and clarity, we take $J_{ls}/J_{qs} = J_l/J_q = 1$) read

$$\beta_s = -1/9(9J_s^2 + 8J_{ls}^2), \quad (3)$$

$$\beta_l = -1/8(12J_l^2 + 9J_{ls}^2), \quad (4)$$

$$\beta_{ls} = -1/6(5J_{ls}^2 + 12J_{ls}J_s + 18J_{ls}J_l), \quad (5)$$

$$\beta_p = 0. \quad (6)$$

There are several points worth stressing. (i) The mixed terms J_{ls} drive the spin and orbital coupling constants to ∞, hence to a fully screened Fermi liquid regime. (ii) If the mixed terms are initially 0, they remain 0 under the RG flow (a conclusion that holds to all orders, as revealed by the NRG results discussed later). (iii) For $J_{ls} = 0$, the spin and orbital moments in the equations above decouple. In that limit, the running of orbital coupling constant is faster, which is associated with a higher SU(3) symmetry. (In contrast to the RG equations, NRG results show that even for vanishing J_{ls} the spin- and orbital- moments are still coupled, for instance, the spin-Kondo temperature depends also on J_l and is not simply exponential in J_s as the equations above suggest.)

NRG results – Fig. 1 shows the impurity contribution to entropy (top panel) and the spin and orbital susceptibilities χ (bottom panel). In the realistic Kondo model the entropy smoothly drops from the value $2\ln 3$ characteristic of freely fluctuating spin and orbital moments (for $S=1$, $L=1$), without any pronounced features. It is only by looking separately at the spin and orbital susceptibilities that the two-stage screening process becomes apparent.

To reveal the physics more clearly, it is convenient to suppress the mixed spin-orbital terms. This separates the spin and orbital Kondo scales further so that the intermediate temperature state is visible also in the impurity contribution to the entropy. A shoulder appears (dashed curve) that becomes more pronounced and takes the form of a clear plateau if the spin Kondo constant is further suppressed (dotted). Now, there is a salient point. Naively, one might expect that the value of the impurity contribution to entropy at the plateau to be $\log 3$, corresponding to fluctuating spins. The calculated entropy at the plateau is, however, larger.

In order to understand the underlying physics, we further simplify the model. First, because the splitting between quadrupole and orbital terms is irrelevant in the RG sense, as shown in the earlier work [21] and as dis-

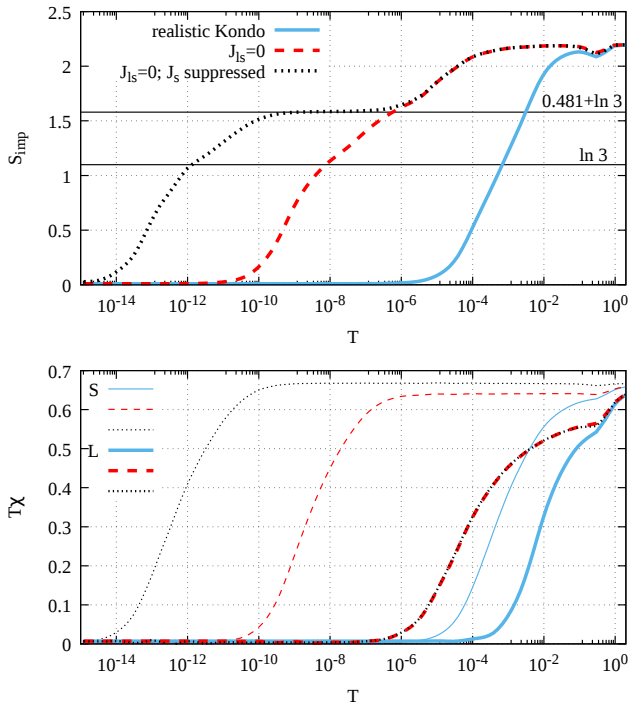

FIG. 1. (top) Impurity contribution to entropy for the Kondo model corresponding to an Anderson model of a realistic impurity (full), the case with vanishing mixed couplings $J_{ls} = J_{qs} = 0$ (dashed), and the case with additionally suppressed spin-Kondo coupling from $J_s = 0.025$ to $J_{ss} = 0.00025$ (dotted). (bottom) The corresponding orbital (thick) and spin (thin) effective moments.

cussed above, one can consider a problem with the higher SU(3) symmetry [19, 20, 24]. Second, because in the state of our interest the spins are freely fluctuating, one can neglect the spin-coupling Kondo constant altogether and set $J_s = 0$. The intermediate temperature behavior at the plateau thus corresponds to a problem described by the interaction Hamiltonian $H_K = T \cdot t$ where T, t are SU(3) objects. The same conduction band orbital moment t is, however, realized by two spin channels (spin plays the role of spectator, as it does not appear in the simplified H_K explicitly), hence the relevant fixed point is that of the impurity with SU(3) orbital degree of freedom coupled to two conduction channels. This problem is overscreened, hence a non-Fermi liquid.

The general overscreened impurity problem with SU(N) symmetry coupled to K conduction channels was explored in the literature in detail [32]. Equation (6) of the cited reference reads

$$S_{\rm imp} = \ln \prod_{n=1}^{Q} \frac{\sin\left[\pi(N+1-n)/(N+K)\right]}{\sin\left[\pi n/(N+K)\right]}, \qquad (7)$$

with $N = 3, K = 2, Q = 2$ in the present case, which

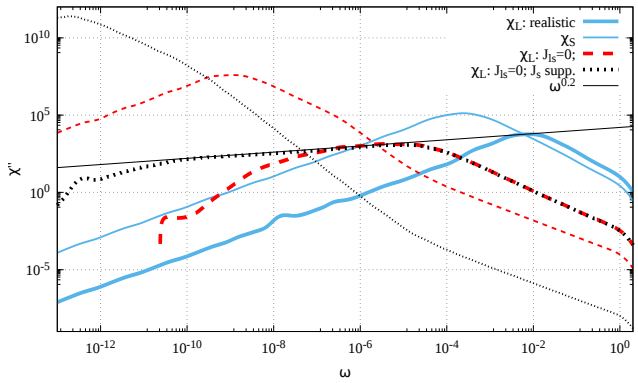

FIG. 2. Frequency dependence of the imaginary part of spin (thin) and orbital (thick) susceptibilities for parameters as in Fig. 1. The realistic result was multiplied by a constant.

evaluates to

$$S_{\rm imp0} = (1/2)\log\left(\frac{3+\sqrt{5}}{2}\right) \approx 0.481 \qquad (8)$$

Adding the ln(3) contribution of the fluctuating spin entropy to that number one obtains 1.58, which coincides with the value of the residual entropy at the plateau as shown on Fig. 1.

Once the fixed point is identified, one knows the scaling of the response functions. For the fixed point at hand, $\chi(T) \sim$ const, hence the temperature dependence of local moments resembles a Pauli response one would expect for a Fermi liquid. On the other hand the scaling of the response as a function of frequency is more interesting, namely, one expects [32] $\chi''_L(\omega) \sim \omega^{1/5}$.

Fig. 2 presents the frequency dependence of the imaginary part of spin and orbital susceptibilities $\chi''_{S,L}(\omega)$, respectively. The spin susceptibilities at small frequencies are substantially larger, corresponding to a smaller value of T_K^S (T_K can be read directly from the frequency at which the corresponding susceptibility attains a maximum). In the intermediate frequency regime $T_K^S < \omega < T_K^L$ the frequency dependence of χ''_L is non-Fermi liquid and follows the $\omega^{1/5}$ dependence, which is particularly clear in curves for the parameters with suppressed mixed and spin-Kondo couplings. This demonstrates that the over-screened SU(3) fixed point controls the electron response in this intermediate energy regime.

Spectral functions – Whereas the frequency dependence of the orbital susceptibility reveals the non-Fermi liquid fixed point in the most direct way, it is not a quantity that is easily measured experimentally. Hence we also calculated the impurity spectral function (that is, the T-matrix). We plot the results in Fig. 3 for the Kondo model with realistic parameters obtained from the Schrieffer-Wolff transformation and for the case with suppressed mixed terms, $J_{ls} = J_{qs} = 0$. The result for realis-

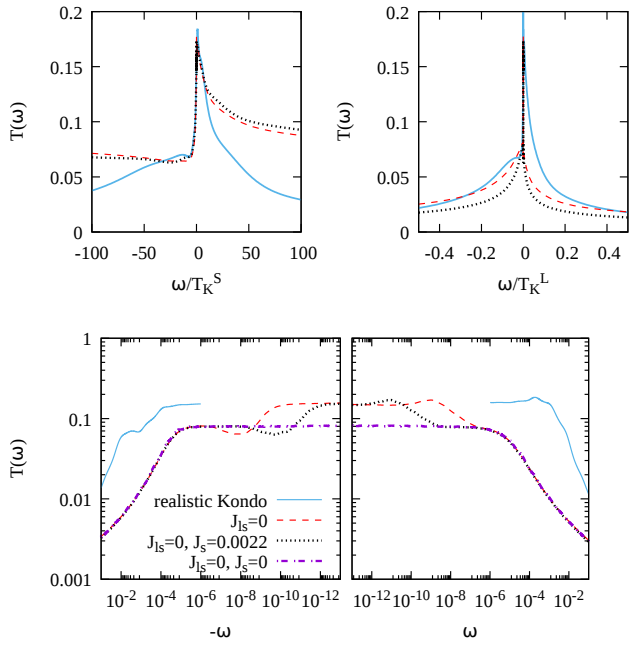

FIG. 3. Frequency dependence of the spectral function $T(\omega)$.

tic parameters reveals asymmetric shape of the quasiparticle peak with a characteristic shoulder (or side-peak) at negative frequency (for the case corresponding to occupancy of two electrons). The shape of the quasiparticle peak was discussed in Ref. 24 as a narrow needle associated with the screening of spin, on a broader hump characteristic of the orbital screening. In earlier work on the Anderson-Kanamori and Hubbard-Kanamori model [33] it was shown that the frequency of the side-peak scales with the coherence scale, that is, for increasing Hubbard repulsion and/or Hund's coupling the feature moves to lower frequencies, which implies that it is not associated with atomic satellites. This inner structure of the quasiparticle peak was (to our knowledge) first discussed in Ref. [34], and is seen in the Anderson-Kanamori model [20].

The present results demonstrate that the side feature is present already in the Kanamori-Kondo model. To explore this in more detail we plot the spectral function on a logarithmic scale (lower panel) for a set of J_s, including the case of $J_s = 0$ that has a non-Fermi-liquid ground state. One sees that the results for finite J_s follow the dependence of the $J_s = 0$ case until approaching the spin-Kondo screening scale. At negative frequencies below the T_K^S the spectral function is first suppressed and then increases as the Fermi liquid coherent state is established.

On this point we also notice that in the case of realistic LDA+DMFT calculation on Sr_2RuO_4 the side-peak is observed at positive frequencies and that its existence was invoked to explain the measured optical

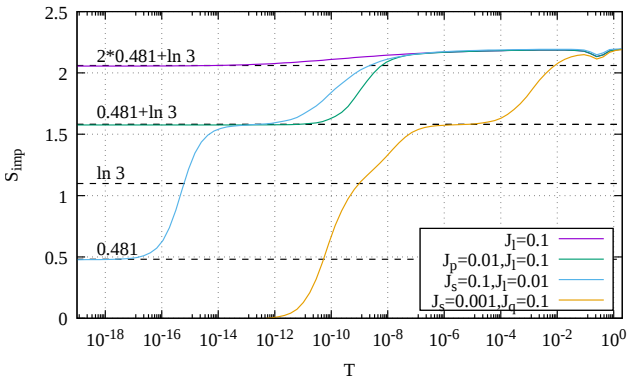

FIG. 4. Temperature dependence of the impurity contribution to entropy. The non-vanishing parameters for respective curves are stated in the legend, the parameters that are not stated explicitly are set to 0.

conductivities[35]. Hence this structure of the quasiparticle peak, that is not present for vanishing Hund's rule coupling, can be considered as a spectral fingerprint of the Hund's metals.

Other non-Fermi liquid regimes – Relaxing the parameters even further one can access additional non-Fermi liquid regimes. The impurity contribution to entropy for some of the interesting cases is shown on Fig. 4 and the corresponding fixed points are listed in Table I. One of the interesting fixed points discussed first in Ref. [36, 37] is that of the case where the quadrupole terms in the Kondo Hamiltonian are suppressed $J_q = J_{qs} = J_{ls} = 0$. In that case, the problem has an additional particle-hole symmetry which reflects the fact that the same spin and orbital moments can be obtained either by 2 or 4 electrons in the impurity (and the matching configuration of bath electrons). This particle-hole symmetry is broken by explicit potential scattering $J_p n$ and also by quadrupole terms $J_q \mathbf{Q} \cdot \mathbf{q}$.

TABLE I. NFL fixed points relevant to Fig. 4; $S_{\rm imp0} = (1/2)\log\left(\frac{3+\sqrt{5}}{2}\right) \approx 0.481$.

when	residual entropy	case
$J_{l(q)s} = 0,\ J_s = 0$	$\ln 3 + S_{\rm imp0}$	two-ch. SU(3)+free spin
$J_q = J_{l(q)s} = J_p = 0$	$S_{\rm imp0}$	three-ch. SU(2)
only $J_l > 0$	$2S_{\rm imp0} + \ln 3$	combination of two above

When those terms are suppressed, the low-energy physics (once the spin is screened) is that of a hypercharge $Y = 1/2$ coupled to three conduction bands given by orbital degrees of freedom and hence to a three-channel over-screened $Y = 1/2$ problem [36]. For that problem, the residual entropy evaluates to $S_{\rm imp1} = 0.481$ (which is, incidentally, the same as earlier discussed $S_{\rm imp0}$), and is the zero-temperature value residual entropy for the case of $J_s = 0.1, J_l = 0.01$ of Fig. 4. In

that case, the spin is fully screened, but the hyper-charge fluctuations lead to the physics just discussed. If the quadrupole terms are retained (case $J_s = 0.1, J_q = 0.01$), the particle-hole symmetry is broken and this physics is not realized. If one suppresses the spin Kondo coupling constant (case where only $J_l = 0.1$ is non-vanishing), the spin is freely fluctuating (the contribution to entropy ln3), and one has a simultaneous occurrence of two-channel over-screened SU(3) problem in the orbital sector and the three-channel over-screened SU(2) problem in the hyper-charge sector, hence one reaches $2 \times 0.481 + \ln 3$ residual entropy. Adding the potential scattering (case $J_p = 0.01, J_l = 0.1$) suppresses the particle-hole symmetry, and the residual entropy is that of the over-screened problem in the orbital sector only.

Studying the frequency dependencies of the corresponding correlation functions for the cases just discussed is an interesting subject for the future work.

Summary – We have revealed a non-Fermi-liquid fixed point that corresponds to the idealized incoherent state of three-orbital Hund's metals within the DMFT description. At energies controlled by this fixed point the orbital susceptibility has an unusual $\omega^{1/5}$ dependence and the spectral function is roughly constant which manifests as a side peak at negative (positive) frequencies for $N_d = 2$ ($N_d = 4$, related to the optical observations on Sr_2RuO_4 [35]). It may be that because within the Anderson model the mixed terms are necessarily larger $J_{ls}/J_l > 1$ the revealed fixed point is not approached closely, but also in that case the presented results provide a useful precise reference point for further discussion.

It would be interesting to develop experimental techniques to investigate the frequency dependent orbital susceptibility, for instance in ruthenates, especially on approaching the half-filled configuration where one can expect a larger separations between the spin- and the orbital coupling scales [21].

A. H., R. Ž., and J. M. are supported by Slovenian Research Agency (ARRS) under Program P1-0044 and Project J1-7259. We warmly thank Antoine Georges for the discussions in particular the ones related to Ref. [32].

[1] A. W. Tyler, A. P. Mackenzie, S. Nishizaki, and Y. Maeno, Phys. Rev. B **58**, R10107 (1998).

[2] Y. S. Lee, J. Yu, J. S. Lee, T. W. Noh, T.-H. Gimm, H.-Y. Choi, and C. B. Eom, Phys. Rev. B **66**, 041104 (2002).

[3] L. Capogna, A. P. Mackenzie, R. S. Perry, S. A. Grigera, L. M. Galvin, P. Raychaudhuri, A. J. Schofield, C. S. Alexander, G. Cao, S. R. Julian, and Y. Maeno, Phys. Rev. Lett. **88**, 076602 (2002).

[4] S. Kamal, D. M. Kim, C. B. Eom, and J. S. Dodge, Phys. Rev. B **74**, 165115 (2006).

[5] M. Schneider, D. Geiger, S. Esser, U. S. Pracht, C. Stingl, Y. Tokiwa, V. Moshnyaga, I. Sheikin, J. Mravlje, M. Scheffler, and P. Gegenwart, Phys. Rev. Lett. **112**, 206403 (2014).

[6] A. Georges, L. d. Medici, and J. Mravlje, Annu. Rev. Condens. Matter Phys. **4**, 137 (2013).

[7] A. Georges, G. Kotliar, W. Krauth, and M. J. Rozenberg, Rev. Mod. Phys. **68**, 13 (1996).

[8] J. Mravlje, M. Aichhorn, T. Miyake, K. Haule, G. Kotliar, and A. Georges, Phys. Rev. Lett. **106**, 096401 (2011).

[9] L. deMedici, J. Mravlje, and A. Georges, Physical Review Letters **107** (2011), 10.1103/physrevlett.107.256401.

[10] K. Haule and G. Kotliar, New J. Phys. **11**, 025021 (2009).

[11] Z. P. Yin, K. Haule, and G. Kotliar, Nat. Mater. **10**, 932 (2011).

[12] A. Isidori, M. Berović, L. Fanfarillo, L. de' Medici, M. Fabrizio, and M. Capone, Phys. Rev. Lett. **122**, 186401 (2019).

[13] A. A. Khajetoorians, M. Valentyuk, M. Steinbrecher, T. Schlenk, A. Shick, J. Kolorenc, A. I. Lichtenstein, T. O. Wehling, R. Wiesendanger, and J. Wiebe, Nature Nanotechnology **10**, 958 (2015).

[14] H. Ishida and A. Liebsch, Phys. Rev. B **81**, 054513 (2010).

[15] T. Misawa, K. Nakamura, and M. Imada, Phys. Rev. Lett. **108**, 177007 (2012).

[16] L. de' Medici, G. Giovannetti, and M. Capone, Phys. Rev. Lett. **112**, 177001 (2014).

[17] J. Steinbauer, L. de' Medici, and S. Biermann, (2019), arXiv:1907.05365.

[18] Z. P. Yin, K. Haule, and G. Kotliar, Phys. Rev. B **86**, 195141 (2012).

[19] C. Aron and G. Kotliar, Physical Review B **91**, 041110 (2015).

[20] K. M. Stadler, Z. P. Yin, J. von Delft, G. Kotliar, and A. Weichselbaum, Phys. Rev. Lett. **115**, 136401 (2015).

[21] A. Horvat, R. Žitko, and J. Mravlje, Phys. Rev. B **94**, 165140 (2016).

[22] J. Mravlje and A. Georges, Phys. Rev. Lett. **117**, 036401 (2016).

[23] A. Horvat, R. Žitko, and J. Mravlje, Phys. Rev. B **96**, 085122 (2017).

[24] K. M. Stadler, J., G. Kotliar, A. Weichselbaum, and von Delft, Ann. Phys. **405**, 365 (2019).

[25] X. Deng, K. M. Stadler, K. Haule, A. Weichselbaum, J. von Delft, and G. Kotliar, Nature Comm. **10**, 2721 (2019).

[26] I. Okada and K. Yosida, Prog. Theor. Phys. **49**, 1483 (1973).

[27] P. Werner, E. Gull, M. Troyer, and A. J. Millis, Phys. Rev. Lett. **101**, 166405 (2008).

[28] R. Hiraoka, E. Minamitani, R. Arafune, N. Tsukahara, S. Watanabe, M. Kawai, and N. Takagi, Nature Communications **8** (2017), 10.1038/ncomms16012.

[29] R. Bulla, T. A. Costi, and T. Pruschke, Rev. Mod. Phys. **80**, 395 (2008).

[30] R. Žitko, "NRG Ljubljana," nrgljubljana.ijs.si/.

[31] R. Žitko, Comput. Phys. Commun. **182**, 2259 (2011).

[32] O. Parcollet, A. Georges, G. Kotliar, and A. Sengupta, Phys. Rev. B **58**, 3794 (1998).

[33] J. Mravlje, (2016), presented in "What about U" conference, Trieste 2016.

[34] H. Wadati, J. Mravlje, K. Yoshimatsu, H. Kumigashira, M. Oshima, T. Sugiyama, E. Ikenaga, A. Fujimori,

A. Georges, A. Radetinac, K. S. Takahashi, M. Kawasaki, and Y. Tokura, Phys. Rev. B **90**, 205131 (2014).
[35] D. Stricker, J. Mravlje, C. Berthod, R. Fittipaldi, A. Vecchione, A. Georges, and D. van der Marel, Phys. Rev. Lett. **113**, 087404 (2014).
[36] L. de Leo, Ph.D. thesis, SISSA (2004).
[37] L. De Leo and M. Fabrizio, Phys. Rev. Lett. **94**, 236401 (2005).